The Position of Q_B in the Photosynthetic Reaction Center Depends on pH: A Theoretical Analysis of the Proton Uptake upon Q_B Reduction

Antoine Taly,*† Pierre Sebban,† Jeremy C. Smith,* and G. Matthias Ullmann*
*Biocomputing Group, IWR, INF 368, Universität Heidelberg, D-69120 Heidelberg, Germany; and †Centre de Génétique Moléculaire, Avenue de la Terrasse, F-91198 Gif-sur-Yvette, France

ABSTRACT Electrostatics-based calculations have been performed to examine the proton uptake upon reduction of the terminal electron acceptor Q_B in the photosynthetic reaction center of *Rhodobacter sphaeroides* as a function of pH and the associated conformational equilibrium. Two crystal structures of the reaction center were considered: one structure was determined in the dark and the other under illumination. In the two structures, the Q_B was found in two different positions, proximal or distal to the nonheme iron. Because Q_B was found mainly in the distal position in the dark and only in the proximal position under illumination, the two positions have been attributed mostly to the oxidized and the reduced forms of Q_B, respectively. We calculated the proton uptake upon Q_B reduction by four different models. In the first model, Q_B is allowed to equilibrate between the two positions with either oxidation state. This equilibrium was allowed to vary with pH. In the other three models the distribution of Q_B between the proximal position and the distal position was pH-independent, with Q_B occupying only the distal position or only the proximal position or populating the two positions with a fixed ratio. Only the first model, which includes the pH-dependent conformational equilibrium, reproduces both the experimentally measured pH dependence of the proton uptake and the crystallographically observed conformational equilibrium at pH 8. From this model, we find that Q_B occupies only the distal position below pH 6.5 and only the proximal position above pH 9.0 in both oxidation states. Between these pH values both positions are partially occupied. The reduced Q_B has a higher occupancy in the proximal position than the oxidized Q_B. In summary, the present results indicate that the conformational equilibrium of Q_B depends not only on the redox state of Q_B, but also on the pH value of the solution.

INTRODUCTION

The photosynthetic reaction center (RC) is the pigment-protein complex that performs the initial steps of conversion of light energy into electrochemical energy for ATP synthesis (Okamura et al., 2000; Sebban et al., 1995a). The structures of the RCs from *Rhodobacter (Rb.) sphaeroides* (Chang et al., 1991; Ermler et al., 1994; McAuley et al., 2000; Stowell et al., 1997) and *Rhodopseudomonas (Rps.) viridis* (Deisenhofer et al., 1985; Deisenhofer and Michel 1989; Lancaster et al., 2000) have been determined up to a resolution of 2.1 and 2.0 Å, respectively.

The bacterial RC of *Rb. sphaeroides* is composed of three subunits: L, M and H. The L and M subunits have pseudo-twofold symmetry. Both the L and M subunits consist of five transmembrane helices. The H subunit caps the RC on the cytoplasmic side and possesses a single N-terminal transmembrane helix. The RC binds several cofactors: a bacteriochlorophyll dimer, two monomeric bacteriochlorophylls, two bacteriopheophytins, two quinones (Q_A and Q_B), a nonheme iron, and a carotenoid. The nonheme iron lies between the two quinone molecules. The primary electron donor, a bacteriochlorophyll dimer called the special pair, is located near the periplasmic surface of the complex, and the terminal electron acceptor, a quinone called Q_B, is located near the cytoplasmic side.

Submitted June 14, 2002, and accepted for publication September 26, 2002.

Address reprint requests to G. Matthias Ullmann, E-mail: matthias.ullmann@iwr.uni-heidelberg.de.

© 2003 by the Biophysical Society

0006-3495/03/03/2090/09 $2.00

Electron transfer from the special pair to Q_B is initiated by the absorption of light, which induces the excitation of the special pair to its lowest excited electronic state. The electron is subsequently transferred in 200 ps to Q_A via a monomeric chlorophyll and a pheophytin. Q_A^- is oxidized in 20–200 μs by electron transfer to Q_B (Li et al., 1998; Tiede et al., 1996). In the RCs of *Rb. sphaeroides*, Q_A and Q_B are both ubiquinone molecules. However, these two ubiquinone molecules have different properties and different functions. The Q_B binding pocket is richer in polar and ionizable residues than that of Q_A. Although Q_A is a one-electron acceptor and does not protonate directly, Q_B accepts two electrons and two protons to form the reduced Q_BH_2 molecule. Q_B is bound at the level of the lipid headgroups at the cytoplasmic side of the membrane and has no direct contact with the aqueous environment. Protons are delivered from the cytoplasm to Q_B by one or more pathways composed of interdependent hydrogen-bond networks involving titratable residues and water molecules (Baciou and Michel, 1995; Ermler et al., 1994; Gerencser et al., 2002; Lancaster and Michel, 1997; Lancaster et al., 1996; Miksovska et al., 1997; Paddock et al., 2001).

The first reductions of Q_A and of Q_B are accompanied by pK_a shifts of residues that interact with the semiquinone species (Wraight, 1979). The reductions induce substoichiometric proton uptake by the protein. The number of protons taken up by the protein upon reduction of the quinones is an observable directly dependent on the energetics of the system and is also intimately coupled to the thermodynamics of the $Q_A^- \rightarrow Q_B$ electron transfer process (Okamura et al.,

2000; Onufriev et al., 2001). Moreover, it has been proposed that proton uptake and rearrangements after Q_A^- formation could be dynamically coupled to the interquinone electron transfer reaction and may gate this reaction (Brzezinski et al., 1992; Maróti and Osváth, 1997; Tiede and Hanson, 1992). The pH dependence of the proton uptake associated with the formation of Q_A^- and Q_B^- in wild type RCs have been determined for *Rb. sphaeroides* (Maroti and Wraight, 1988; McPherson et al., 1988; Tandori et al., 2002) and *Rb. capsulatus* (Sebban et al., 1995b).

Using x-ray structural analysis, it has been shown that a major conformational difference exists between the RC handled in the dark (the ground state) or under illumination (the charge-separated state) (Stowell et al., 1997). The main difference between the two structures concerns Q_B itself, which was found in two different positions ~4.5 Å apart. In the dark-adapted state in which Q_B is oxidized, Q_B is found mainly in the distal position and only a small percentage in the proximal position. Under illumination, i.e., when Q_B is reduced, Q_B is seen only in the proximal position. The crystal was grown at pH = 8 (Allen, 1994). The reaction center structures with proximal or distal Q_B are called RC^{prox} and RC^{dist}, respectively (Lancaster and Michel, 1997). A similar conformational equilibrium was found for the RC of *Rps. viridis* (Lancaster, 1999a). A schematic representation of this crystallographically observed equilibrium is shown in Fig. 1.

Conformational changes can shift pK_a values of residues in proteins (Beroza and Case, 1998; Gunner and Alexov, 2000; Huang et al., 2002; Mulkidjanian, 1999; Rabenstein and Knapp, 2001). It is therefore interesting to investigate the effect of pH and thus protonation state changes on the conformational equilibria associated with pK_a switching. Conformational equilibria play a central role in the physiological function of many proteins (Graige et al., 1998; Huang et al., 2002; Mulkidjanian, 1999; Rabenstein and Knapp, 2001). For the RC, it was, for instance, proposed that a conformational equilibrium participates in the gating of the first electron transfer between Q_A and Q_B (Graige et al., 1998). A theoretical understanding of the pH dependence of conformation equilibria is therefore of general interest in protein biophysics. This understanding can be approached with the use of the Poisson-Boltzmann equation in which the protein atoms are explicitly represented by partial charges and the environmental effect are included by a continuum description (Honig and Nicholls, 1995; Honig et al., 1989; Sharp et al., 1995; Sharp and Honig, 1990; Yang et al., 1993). This approach allows the computation of the electrostatic potential at any point inside and outside the protein. The electrostatic potential depends on and determines the protonation of the individual residues. Combining Poisson-Boltzmann calculations with Monte Carlo sampling of protonation states allows calculating the overall proton uptake to be performed, together with a decomposition of the contributing residues.

In the calculations presented here, we investigate how the proton uptake upon Q_B reduction in the *Rb. sphaeroides* RC depends on the pH and on the conformational equilibrium of Q_B found experimentally (Stowell et al., 1997). We show that a model, in which the equilibrium between the conformations RC^{prox} and RC^{dist} varies with pH, reproduces the experimentally measured pH dependence of the proton uptake (Tandori et al., 2002) as well as the occupation of RC^{prox} and RC^{dist} observed in the crystallographic study at pH = 8 (Stowell et al., 1997). In the model, the populations of the two conformations in the ground and charge-separated states of the RC are pH dependent. The results of the study provide insight into the balance between the global protein electrostatics and conformational equilibrium of a protein, and how conformational equilibria are controlled by pH.

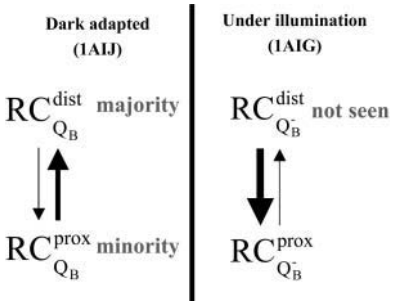

FIGURE 1 Illustration of the crystallographically determined equilibrium (Stowell et al., 1997). The left side represents the structure of dark-adapted RCs, in which Q_B is oxidized. Q_B is seen in two positions: proximal and distal. The structures with proximal and distal Q_B are called RC^{prox} and RC^{dist}, respectively. The right side represents the structure for light-exposed RCs, in which Q_B is reduced. No electron density is observed experimentally for RC^{dist}.

METHODS

Structure preparation

X-ray structures used

The x-ray structures of the dark-adapted (PDB entry 1AIJ) and light-exposed (PDB entry 1AIG) RCs from *Rb. sphaeroides* with resolutions of 2.2 and 2.6 Å (Stowell et al., 1997), respectively, were used in this study. 1AIG was used for all states in which Q_B is in the proximal position; 1AIJ was used for all states in which Q_B is in the distal position.

Structure preparation

Two RCs are present in the asymmetric unit of the crystal. We consider only the first RC structure of the PDB entries 1AIJ and 1AIG, not the second. The second RC in the asymmetric unit is less complete than the first. All explicit water and detergent molecules were removed. The influence of water was represented using a dielectric constant of 80 (Adcock et al., 1998; Baptista and Soares, 2001; Gibas and Subramaniam, 1996; Lancaster et al., 1996; Rabenstein et al., 1998; Teixeira et al., 2002). The use of lower dielectric constants (e.g. 30) inside cavities does not influence protonation probability calculations significantly (Adcock et al., 1998). Therefore, we did not consider this effect. Most of the nonpolar hydrogen atoms were considered as one atom together with the heavy atoms to which they are bound (the extended atom representation). For the quinones, the bacteriochlorophylls, and the bacteriopheophytins all hydrogens were treated explicitly. Polar

hydrogens, i.e., those bound to oxygen, nitrogen, or sulfur atoms, were also treated explicitly, except for the acidic hydrogens of protonated carboxylate groups which were represented by symmetrical charge adjustment of the two carboxyl oxygen atoms (Rabenstein et al., 1998). Coordinates of explicitly treated hydrogen atoms were generated with the HBUILD module (Brunger and Karplus, 1988) in CHARMM (Brooks et al., 1983). The hydrogen atom positions were energy optimized with the heavy-atom positions fixed. For this optimization, all titratable groups were in their standard protonation states (i.e., the aspartate, glutamate and the C-termini were unprotonated; the arginine, cysteine, histidine, lysine, tyrosine and the N-termini were protonated), and both quinones were in their oxidized (uncharged) state. The hydrogen atom positions were kept fixed during the electrostatic calculations. The continuum representation of the water and symmetrical distribution of the charges over the protonatable groups mimics the mobility of the hydrogen atoms and the water molecules well (Gibas and Subramaniam, 1996). This representation is computationally much less demanding than treating these effects explicitly. We used the same atomic partial charges as in previous calculations (Rabenstein et al., 1998, 2000). The charges of bacteriopheophytin and bacteriochlorphyll, which have not been published before, are listed in Supplementary Material.

Proton uptake calculation

Calculation of protonation probabilities

Each protonation state of a protein can be characterized by a protonation state vector $\vec{x}^{n,k} = (x_1^{n,k}, x_2^{n,k}, \ldots, x_\mu^{n,k}, \ldots, x_N^{n,k})$, where the components $x_\mu^{n,k}$ are 1 or 0 depending on whether group μ is protonated or not. The superscripts n and k designate the protonation state and the conformation of the protein, respectively. The energy $G^{n,k}$ of a protonation state n of the protein in a conformation k is given by Eq. 1 (Bashford and Karplus, 1990; Ullmann and Knapp, 1999).

$$G^{n,k} = \sum_{\mu=1}^{N} [(x_\mu^{n,k} - x_\mu^0) RT \ln 10(\mathrm{pH} - (\mathrm{pK}_{a,\mu}^{model} + \Delta\mathrm{pK}_{a,\mu}^{prot,k}))] + 1/2 \sum_{\mu=1}^{N} \sum_{\nu=1}^{N} [W_{\mu\nu}^{k} (x_\mu^{n,k} + z_\mu^0)(x_\nu^{n,k} + z_\nu^0)] + \delta^k \Delta G_{conf}^{k}, \quad (1)$$

where z_μ^0 is the unitless formal charge of the deprotonated form of group μ, i.e., -1 for acids and 0 for bases, and x_μ^0 is the reference protonation state of group μ; $\mathrm{pK}_{a,\mu}^{model}$ is the experimentally known $\mathrm{pK_a}$ value of a model compound of the titratable group (N-formyl N-methylamide derivatives of the respective amino acids) in aqueous solution (Tanford and Roxby, 1972); $\Delta\mathrm{pK}_{a,\mu}^{prot,k}$ is the shift of the model compound $\mathrm{pK_a}$ value of the titratable groups due to the different solvation environment inside the protein (changed dielectric environment and interaction with non-titrating charges); $W_{\mu\nu}^{k}$ is the electrostatic interaction between the titratable groups μ and ν in the conformation k if both are charged; δ^k is 1 or 0 depending on whether the protein is in conformation k or not; R is the universal gas constant, and T is the temperature. ΔG_{conf}^{k} is the free energy difference between conformation k and the reference conformation $k = 0$ in which all sites are in the reference protonation state (Eq. 2). In the present case, the reference conformation $k = 0$ is that with a proximal quinone.

$$\Delta G_{conf}^{k} = G_{conf}^{k} - G_{conf}^{0}. \quad (2)$$

This energy difference refers to the energy of the specific protein conformation and for a specific redox state of Q_B. Here, ΔG_{conf} has two different values, one for each redox state of Q_B: $\Delta G_{conf}^{Q_B^-}$ when Q_B is reduced and $\Delta G_{conf}^{Q_B}$ when Q_B is oxidized. As discussed by others (Rabenstein and Knapp, 2001), the value of ΔG_{conf} is composed of different contributions, such as, for example, van der Waals interactions, and Coulombic interactions between nontitratable groups and titratable groups (the latter being only considered in the reference protonation state), and torsion energies. Accurate determination using theory of each of these contributions, and thus ΔG_{conf}, is difficult. Therefore, it is common practice to treat ΔG_{conf} as an adjustable parameter to reproduce experimental data. Here ΔG_{conf} was kept constant with pH.

The terms $\Delta\mathrm{pK}_a^{prot,k}$ and $W_{\mu\nu}^{k}$ were calculated from the linearized Poisson-Boltzmann equation of a molecular system using a finite difference method with the program MEAD (Bashford and Gerwert, 1992). The Poisson-Boltzmann equation was solved using a three-step grid-focusing procedure (Bashford and Gerwert, 1992; Klapper et al., 1986; Rabenstein et al., 1998) with an initial 250-Å cube with a 2.5-Å lattice spacing centered at the protein, followed by 100-Å cube with a 1.0-Å lattice spacing, and a 45-Å cube with 0.3-Å lattice spacing, both centered at the titratable group. We used an ionic strength of 100 mM, an ion exclusion layer of 2 Å, and a solvent probe radius of 1.4 Å. The dielectric constant of the protein was set to $\varepsilon_P = 4$ and the dielectric constant of the solvent (outside the protein and within protein cavities) was set to $\varepsilon_S = 80$.

The average protonation probability of each titratable group was calculated by a Monte Carlo procedure (Beroza et al., 1991) using the program Karlsberg (Rabenstein and Knapp, 2001; Rabenstein et al., 2000). For the histidines, two tautomers were considered explicitly. All other titratable groups were treated by a single tautomer, which represented an average over all possible tautomers. In previous studies, this approach gave good agreement with experimentally determined $\mathrm{pK_a}$ values (Bashford et al., 1993; Rabenstein and Knapp, 2001; Rabenstein et al., 1998, 2000; Ullmann, 2000). The Monte Carlo sampling was sufficient to reach a standard deviation of less than 0.01 proton at each individual titratable group. Most of the standard deviations were much smaller than 0.01. The sum of the standard deviations of all protonation probabilities was ~0.02 proton.

Proton uptake calculation

The protonation probabilities of the 172 titratable residues were computed for the states Q_AQ_B and $Q_AQ_B^-$. The protonation probability difference between the states Q_AQ_B and $Q_AQ_B^-$ was directly compared to the corresponding experimental data. The experimental pH dependence of the proton uptake determined by Tandori et al., 2002 and McPherson et al., 1988 are very similar. In plots presented in this paper, the experimental data from Tandori et al., 2002 are used for comparison with the calculations. Four different models were used for the proton uptake calculations:

In Model 1 (Fig. 2 *a*), the conformational equilibrium and redox states are pH dependent. Four possible redox and conformational states of the RC are included: oxidized Q_B in the proximal position (RC_{QB}^{prox}), reduced Q_B in the proximal position (RC_{QB-}^{prox}), oxidized Q_B in the distal position (RC_{QB}^{dist}), and reduced Q_B in the distal position (RC_{QB-}^{dist}). In the model, each of these redox and conformational states exists in 2^N protonation states where N is the number of protonation sites. These states are in thermodynamic equilibrium, i.e., they are populated with the Monte Carlo method according to Boltzmann statistics. ΔG_{conf} was adjusted such that both the experimentally determined pH dependence of the proton uptake (Tandori et al., 2002) and the crystallographically determined equilibrium between the two structures observed at pH = 8 (Stowell et al., 1997) were simultaneously reproduced. This agreement was achieved as follows: the difference between the calculated and experimental pH dependence of the proton uptake was minimized subject to two constraints: i), the occupancy of the RC^{prox} conformation was constrained to be lower than 50% when Q_B is oxidized, and ii), when Q_B is reduced, the occupancy of the RC^{prox} structure should be at least 70%. These two constraints ensure that the results are consistent with the observations made crystallographically (Stowell et al., 1997). The values obtained for the conformational energy difference are $\Delta G_{conf}^{Q_B^-} = 1.20$ eV and $\Delta G_{conf}^{Q_B} = 1.23$ eV. The values found here are of the same order as in previous studies (Rabenstein and Knapp, 2001).

Model 2 (Fig. 2 *b*) allows one to test if the conformational equilibrium is pH dependent or not. To do this, the populations of RC^{prox} and RC^{dist} are fixed and constant over the whole pH range for each quinone redox state.

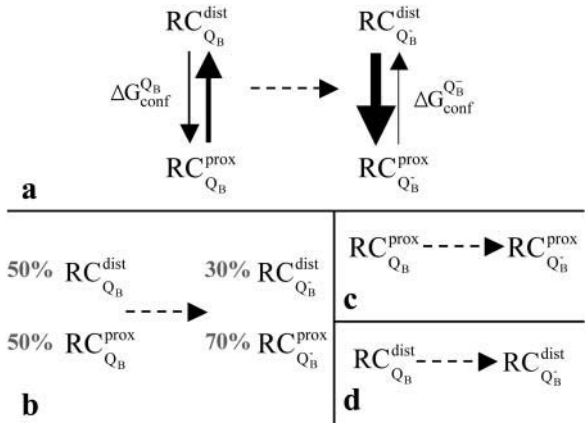

FIGURE 2 Illustration of the four models used to test the relationship between RC conformations and proton uptake upon reduction of Q_B. (*a*) Model 1 describes a pH-dependent conformational equilibrium between RC^{prox} and RC^{dist} for Q_B and Q_B^-. (*b*) Model 2 uses the populations of RC^{prox} and RC^{dist} for Q_B and Q_B^- found with the first model at pH 8 and keeps the ratio of the different conformations constant over the whole pH range. (*c*) Model 3 uses only the RC^{prox} structure for both redox states of Q_B over the whole pH range. (*d*) Model 4 uses only the RC^{dist} structure for both redox states of Q_B over the whole pH range.

The populations used are those determined at pH = 8 with Model 1 (i.e., those consistent with the crystallographic results obtained at pH 8).

In Model 3 (Fig. 2 *c*) and Model 4 (Fig. 2 *d*) only a single structure, RC^{prox} or RC^{dist} respectively, is used in the calculations. Therefore, in both of these models Q_B is in the same position over the whole pH range, whether reduced or not. Model 3 and Model 4 are used to test if a single conformation is sufficient to reproduce the experimental pH dependence of the proton uptake.

RESULTS AND DISCUSSION

The aim of the present work is to understand the pH dependence of the proton uptake associated with the reduction of Q_B and its relation to the experimentally observed conformational equilibrium. Four models were compared to two sets of experimental data: the conformational equilibrium between the RC^{prox} and RC^{dist} structures found at pH = 8 by x-ray crystallography (Stowell et al., 1997) and the pH dependence of the proton uptake upon Q_B reduction (Tandori et al., 2002).

The structural equilibrium found crystallographically (Stowell et al., 1997) is schematically shown in Fig. 1. In the dark-adapted RC (*left side* of Fig. 1), Q_B is found in the two positions with a majority in the distal position. In contrast, no electron density was observed for Q_B in the distal position in the light-exposed RC. This observation implies that under light illumination when Q_B is reduced, the proportion of RC with distal Q_B is very low at pH 8 where the structure was determined.

Proton uptake calculations with different models

The proton uptake upon Q_B reduction was calculated with four different models as described in the Methods section. The results are compared with the experimentally measured proton uptake curves.

Model 1: pH- and redox-dependent equilibrium between RC^{prox} and RC^{dist}

Model 1 is shown in Fig. 2 *a*. In this model, the RC adapts two conformations, RC^{prox} and RC^{dist}, in both oxidation states of Q_B. The equilibrium between the two conformations was adjusted to fit the experimental proton uptake data by varying ΔG_{conf}. The model implies that when Q_B is neutral both structures are equally populated at pH = 8. In contrast, RC^{prox} is 70% occupied at pH = 8 when Q_B is reduced. Changing the population probabilities of the two positions to other rations which are also in agreement with crystallographic data led to the same behavior of the proton uptake curve, i.e., first a decrease of the proton uptake followed by an increase, but with worse overall agreement with the proton uptake data. The equilibrium found from the fits describes the pH dependence of the proton uptake and the crystallographically observed conformational equilibrium well.

In the neutral pH range, the population of RC^{prox} is higher when Q_B is reduced than when it is oxidized, as was imposed for consistency with the x-ray observations (Stowell et al., 1997). The shift of the equilibrium between RC^{prox} and RC^{dist} upon Q_B reduction is somewhat smaller in the calculations than seen crystallographically. However, the difference between the calculated equilibrium and the one seen by x-ray crystallography corresponds to a small energy difference of the order of the thermal fluctuation energy ($k_BT \sim 0.6$ kcal/mol), which is well within the error of the method.

The experimental pH dependence of the proton uptake presented in Fig. 3 *a* decreases from pH 6 to 8 and increases above pH 8 to reach a plateau above pH 9. The calculated proton uptake reproduces this shape. Therefore, Model 1, which allows a pH-dependent structural equilibrium between RC^{prox} and RC^{dist} for Q_B and Q_B^-, is capable of satisfactorily describing the pH dependence of the proton uptake.

Fig. 3 *b* shows the pH dependence of the equilibrium between RC^{prox} and RC^{dist} as a function of pH for both redox states of Q_B, resulting from Model 1. In both states, Q_AQ_B and $Q_AQ_B^-$, the occupancy of the RC^{prox} structure increases with increasing pH.

The results indicate that the structural equilibrium between the conformations RC^{prox} and RC^{dist} depends on both the redox state of Q_B and the pH value of the solution. Model 1 indicates that the structural transition is controlled by the redox state of Q_B only in the pH range between 6.5 and 8.5. At lower or higher pH the equilibrium is totally shifted to the conformations RC^{dist} or RC^{prox}, respectively.

It is known from experiments that Q_B is loosely bound at high pH. The experimental proton uptake data, with which we compare our results, are corrected for this effect (Tandori et al., 2002). Our calculations indicate that at high pH the

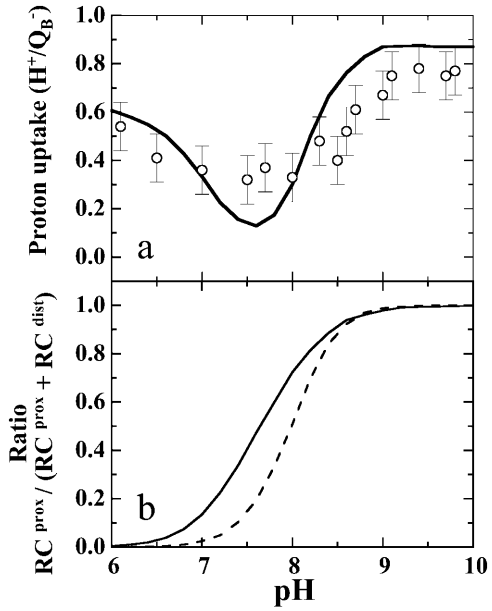

FIGURE 3 (*a*) Proton uptake upon reduction of Q_B, calculated using Model 1, which considers a conformational equilibrium between RC^{prox} and RC^{dist} for Q_B and Q_B^- is shown by the black line. The experimental proton uptake at the different pH values are shown by gray circles. (*b*) Equilibrium between RC^{prox} and RC^{dist} structures. The calculated ration $RC^{prox}/(RC^{prox} + RC^{dist})$ is shown for oxidized (*dashed line*) and reduced (*solid line*) Q_B.

proximal position of Q_B is favored relative to the distal position independent of the redox state of Q_B and the occupation of the Q_B site.

Decomposition of the proton uptake in Model 1

The global proton uptake can be decomposed into two major contributions, which are shown in Fig. 4. The proton uptake is mainly due to residues Glu-L212 and Asp-L213. At pH 7 the proton uptake due to Glu-L212 is calculated to be 0.54, in reasonable agreement with the value of ~0.3–0.4 obtained from FTIR experiments (Nabedryk et al., 1995). According to our results, the residues Asp-L210 and Glu-H173 do not change their protonation probability significantly upon Q_B reduction. In the neutral pH range, the difference between the proton uptake of the residues Glu-L212 and Asp-L213 and the total proton uptake arises from the conformational change that is accompanied by small changes of protonation probabilities of several residues (Arg-M136, Asp-M17, Glu-H33, Glu-M236, His-H116, His-H118, Lys-H50, Lys-H52, Lys-H136, Lys-H187, Lys-H222). The residues that are in contact with the membrane region do not participate in the proton uptake.

The total protonation probability of the RC is higher in conformation RC^{dist} than in the conformation RC^{prox}. Thus, RC^{dist} is stabilized at low pH and RC^{prox} at high pH. However, Glu-L212 and Asp-L213 are more protonated in the RC^{prox} conformation (Table 1) even at low pH. Other residues listed in the previous paragraph change their protonation

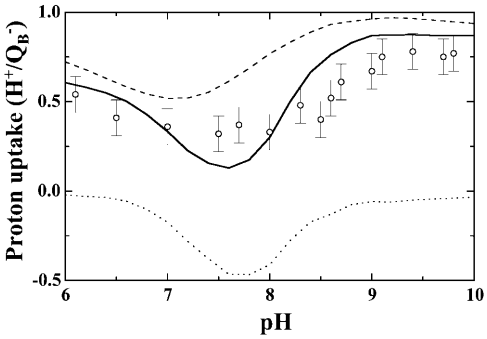

FIGURE 4 Decomposition of the proton uptake obtained with Model 1. Experimental proton uptake is shown by gray circles, total proton uptake by a solid line, contribution of residues GLU-L212 and ASP-L213 by a dashed line, and the contribution of the remaining residues, which are listed in the main text, are shown by a dotted line.

because of the conformational transition and thus compensate for this effect. The titration of Glu-L212 and Asp-L213 is irregular (Table 1). Such an irregular titration behavior is indicative of complicated electrostatic interaction and has been also observed for other molecules (Onufriev et al., 2001; Sudmeier and Reilley, 1964; Zuiderweg et al., 1979).

Model 2: pH-independent, redox-driven transition between RC^{prox} and RC^{dist}

This model was designed to test the hypothesis that structural rearrangement might be driven solely by the change of redox state of Q_B. According to this hypothesis, the position of Q_B changes when Q_B is reduced, independent of the pH. The calculations were therefore performed with the populations of RC^{prox} and RC^{dist} imposed at the values found with Model 1 at pH = 8 over the whole pH range, i.e., 50% RC^{prox} when Q_B is oxidized and 70% RC^{prox} when Q_B is reduced. The proton uptake in the pH range from 6 to 10 calculated using Model 2 is shown in Fig. 5 *a*. Clearly, this model cannot qualitatively reproduce the variation with pH of the experimental proton uptake upon Q_B reduction. The calculated proton uptake is in good agreement with experiments in the pH range from 6.5 to 8.5. However, outside the range from 6.5 to 8.5, there is clear deviation from experiment. This disagreement is a further indication that the conformational equilibrium between RC^{prox} and RC^{dist} is

TABLE 1 Protonation probability of Glu-L212 and Asp-L213 when Q_B is reduced calculated for the conformations RC^{dist} and RC^{prox} and for Model 1

		pH		
Residue	Q_B position	6.0	8.0	10.0
Glu-L212	RC^{prox}	1.0	1.0	1.0
	RC^{dist}	0.78	0.3	0.27
	Model 1	0.78	0.82	1.0
Asp-L213	RC^{prox}	1.0	0.99	0.92
	RC^{dist}	0.89	0.85	0.77
	Model 1	0.89	0.94	0.92

pH dependent, and that Q_B changes its equilibrium position after reduction only in the pH range from 6.5 to 8.5.

Model 3: fixed conformation RC^{prox}

In this model, the RC^{prox} structure was used for both redox states of Q_B over the whole pH range (Fig. 2 *c*). The pH dependence of the proton uptake upon reduction of Q_B calculated using this model is displayed in Fig. 5 *b*. This model is in agreement with experiments only around pH 6 and between pH 9 and 10 but cannot reproduce either the experimentally observed decrease in proton uptake between pH 6 and 8 or the increase between pH 8 and 9. The agreement between calculated and experimental proton uptake in the pH range from pH 9 to 10 is consistent with the results obtained from Model 1, because the RC^{prox} structure satisfactorily represents the RC in both redox states in the pH range from 9 to 10. According to Model 1, only RC^{prox} is populated above pH 9.

Model 4: fixed conformation RC^{dist}

In Model 4, the RC^{dist} structure was used for both redox states of Q_B over the whole pH range (Fig. 2 *d*). The pH-dependent proton uptake calculated from this model is shown in Fig. 5 *c*. The model reproduces well the experimental proton uptake below pH = 8. However, above pH = 8, the results from Model 4 do not even qualitatively follow the experimental data. This finding is again in agreement with Model 1, because the RC populates only the RC^{dist} conformation at low pH for both Q_B and Q_B^-.

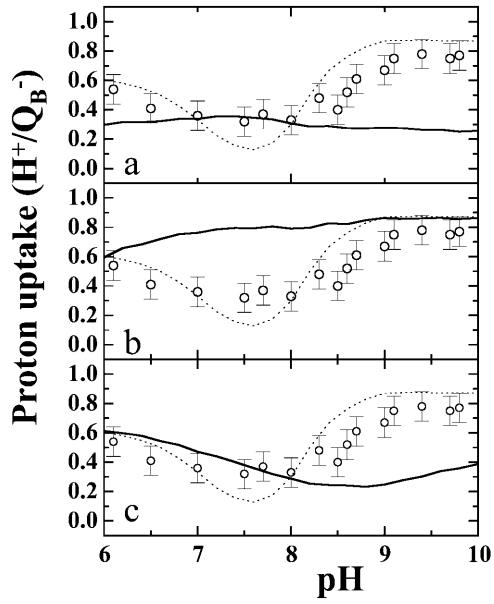

FIGURE 5 Proton uptake of the RC upon reduction of Q_B. Comparison of calculated (*solid line*) and experimental data (*circles*). The calculations were performed with (*a*) Model 2. (*b*) Model 3. (*c*) Model 4. The proton uptake of Model 1 is shown as a dotted line for comparison.

Comparison of the four models

Only Model 1, which includes a pH-dependent structural equilibrium between the RC^{prox} and RC^{dist}, describes the proton uptake experiments satisfactorily over the whole pH range. We therefore conclude that a pH-dependent structural equilibrium between RC^{prox} and RC^{dist} is necessary to describe the pH dependence of the proton uptake upon Q_B reduction. Models 2, 3, and 4 describe the experimental data well over limited pH ranges over which they are found to be valid approximations to Model 1.

Relation to previous calculations

Several theoretical studies on protonation probabilities and conformational changes in the Q_B pocket of different RCs have be done before (Alexov et al., 2000; Alexov and Gunner, 1999; Grafton and Wheeler, 1999; Lancaster et al., 1996; Lancaster, 1999b; Rabenstein et al., 1998, 2000; Walden and Wheeler, 2002; Zachariae and Lancaster, 2001). However, none of these studies considered the pH dependence of the conformational transition between RC^{prox} and RC^{dist}. Here, we make that connection and corroborate our calculation by reproducing experimental proton uptake measurements.

A previous study used only one structure in the evaluation of the proton uptake (Beroza et al., 1995). In this structure (PDB entry 4RCR), Q_B is in the proximal site. The proton uptake calculated in this study (Beroza et al., 1995) is within 0.05 proton of the results obtained in the present work using only the RC^{prox} structure over the whole pH range (i.e., Model 3).

The way flexibility is treated in Model 1 differs from previous calculations in which the flexibility was introduced by allowing the side chains of 26 residues to occupy the different conformations found in the different x-ray structures of the RC protein (Alexov and Gunner, 1999). In addition, Q_B was allowed to occupy the distal and proximal positions. This model involves a large number of possible conformational substates and thus also many parameters to describe them. The calculations done with this model reproduced the pH dependence of proton uptake, but the pH dependence of the quinone position occupancy was not reported.

Interestingly, according to our calculations, residues Glu-L212 and Asp-L213 are protonated from pH 6 to 10 when Q_B is reduced and proximal. A study using molecular dynamics simulation has shown that the proximal position of Q_B^- is more stable when both residues Glu-L212 and Asp-L213 are protonated (Grafton and Wheeler, 1999). The present study is therefore in agreement with this work. However, the results obtained in the present study suggest that the position of Q_B does not depend only on the protonation state of L212 and L213, but also on the protonation state of other residues that trigger the conformational transition between RC^{prox} and RC^{dist}. This finding is also sup-

ported by a more recent study (Walden and Wheeler, 2002). It should, however, be mentioned that in those theoretical studies (Grafton and Wheeler, 1999; Walden and Wheeler, 2002) Q_B occupies the proximal position in an orientation that has never been found crystallographically (McAuley et al., 2000; Zachariae and Lancaster, 2001)

Molecular dynamics simulations of the RC of *Rps. viridis* have provided evidence supporting the movement of Q_B between the distal site and the proximal site (Zachariae and Lancaster, 2001). This work showed that the equilibrium between the two binding sites is not only displaced by the reduction of Q_B to the semiquinone, but also by the preceding reduction of the primary quinone Q_A and accompanying protonation changes in the protein. The present model supports this idea, because the position of Q_B is influenced by the protonation states of the residues surrounding Q_B which may in turn be influenced by the redox state of Q_A (Zachariae and Lancaster, 2001).

CONCLUSIONS

The aim of the present study was to understand the pH dependence of the proton uptake associated with the reduction of Q_B. Two experimentally observed conformations of the RC were considered: with Q_B bound in the proximal or the distal binding site. Comparing the calculated and experimental pH dependence of the proton uptake reveals that a pH-dependent conformational transition is required to reproduce the experimental proton uptake curve. Neither the individual conformations nor a static mixture of the two conformations with a pH-independent population are capable to reproduce the experimental proton uptake profile. The present study presents a new picture in which the position of Q_B depends not only on the redox state of Q_B, but also on pH. This hypothesis could be tested experimentally, for instance by x-ray crystallography at different pH values.

The kinetics of the first electron transfer reaction between Q_A and Q_B is biphasic (~20–60 μs and 150–400 μs) (Li et al., 1998; Tiede et al., 1996). Both electron transfer rates are gated, i.e., not limited by the electron transfer process itself but by other processes (Graige et al., 1998; Hoffman and Ratner, 1987; Ullmann et al., 1997; Zhou and Kostic, 1993). The conformational transition of Q_B from the distal to the proximal sites has been proposed to be one of the rate limiting steps of the first electron transfer (Graige et al., 1998).

Because of the observation that Q_B occupies the proximal position when it is reduced (Stowell et al., 1997), i.e., after the electron transfer, the proximal position has been suggested to be active for electron transfer and the distal position to be inactive (Graige et al., 1998). However, a proximal position of Q_B is not necessarily associated with a nongated electron transfer (Ädelroth et al., 2000; Kuglstatter et al., 2001; Tandori et al., 2002). Consequently, when Q_B is proximal other processes may also gate the first electron transfer from Q_A to Q_B. However, if the movement of Q_B is one of the rate limiting steps, our results imply that the proportion of RCs for which the first electron transfer between Q_A and Q_B is gated by the movement of Q_B will decrease with increasing pH. This idea will be tested in future theoretical and experimental studies.

SUPPLEMENTARY MATERIAL

S1 Partial charges of Bacteriopheophytin, calculated by a semi-empirical method. Atom numbers are according to the PDB file IAIG

Atom name	Charge	Atom name	Charge	Atom name	Charge	Atom name	Charge
NA	−0.49	1HAA	0.02	C5	0.00	C3C	−0.22
NB	−0.5	2HAA	0.02	H8	0.00	CAC	−0.11
HNB	0.36	C3A	−0.22	H9	0.00	2HAC	0.07
NC	−0.35	H3A	0.07	C6	0.00	CBC	0.08
ND	0.52	CMA	0.00	H10	0.00	2HBC	0.00
HND	−0.01	1HMA	0.01	H11	0.00	3HBC	0.00
C1A	−0.02	2HMA	0.01	C2B	−0.04	1HBC	0.00
CHA	0.11	3HMA	0.01	CMB	−0.02	C2D	0.05
C4D	−0.15	CBA	−0.3	1HMB	0.03	CMD	0.05
C1B	0.44	2HBA	0.1	2HMB	0.03	1HMD	0.01
CHB	−0.65	1HBA	0.1	3HMB	0.03	2HMD	0.01
HHB	0.21	CGA	0.79	C3B	−0.39	3HMD	0.01
C4A	0.56	O1A	−0.54	CAB	0.79	C3D	−0.43
C1C	0.28	O2A	−0.43	OBB	−0.52	CAD	0.89
CHC	−0.46	C1	0.19	CBB	−0.41	OBD	−0.55
HHC	0.17	H1	0.01	HB1	0.11	CBD	−0.8
C4B	0.4	H2	0.01	HB2	0.11	1HBD	0.3
C1D	−0.25	C2	0.00	HB3	0.11	CGD	0.98
CHD	−0.2	H3	0.00	C2C	0.17	OID	−0.53
HHD	0.2	C3	0.00	H2C	0.02	O2D	−0.49
C4C	0.17	C4	0.00	CMC	−0.09	CED	0.27
C2A	0.14	H5	0.00	1HMC	0.03	1HED	−0.02
H2A	0.06	H6	0.00	2HMC	0.03	2HED	−0.02
CAA	0.06	H7	0.00	3HMC	0.03	3HED	−0.02
NA	0.11	CAA	−0.13	H7	0.00	2HAC	0.08
NB	0.12	1HAA	0.09	C5	0.00	CBC	0.11
NC	0.01	2HAA	0.09	H8	0.00	2HBC	0.00
ND	0.01	C3A	−0.04	H9	0.00	3HBC	0.00
C1A	0.03	H3A	0.06	C2B	−0.16	1HBC	0.00
CHA	−0.22	CMA	0.01	CMB	0.11	C2D	0.18
C4D	0.21	1HMA	0.01	1HMB	−0.01	CMD	−0.03
C1B	−0.05	2HMA	0.01	2HMB	−0.01	1HMD	0.03
CHB	−0.2	3HMA	0.01	3HMB	−0.01	2HMD	0.03
HHB	0.19	CBA	−0.21	C3B	−0.32	3HMD	0.03
C4A	−0.1	2HBA	0.08	CAB	0.65	C3D	−0.41
C1C	−0.19	1HBA	0.08	OBB	−0.57	CAD	0.81
CHC	−0.17	CGA	0.77	CBB	−0.14	OBD	−0.52
HHC	0.2	O1A	−0.53	HB1	0.04	CBD	−0.73
C4B	−0.02	O2A	−0.42	HB2	0.04	1HBD	0.29
C1D	−0.06	C1	0.15	HB3	0.04	CGD	1.04
CHD	−0.13	H1	0.01	C2C	0.24	O1D	−0.57
HHD	0.18	H2	0.01	H2C	−0.01	O2D	−0.5
C4C	0.05	C2	0.00	CMC	−0.05	CED	0.19
C2A	0.1	H3	0.0	1HMC	0.02	1HED	0.00
H2A	0.05	C3	0.0	2HMC	0.02	2HED	0.00
CAA	−0.13	C4	0.0	3HMC	0.02	3HED	0.00
1HAA	0.09	H5	0.0	C3C	−0.12	MG	0.0
2HAA	0.09	H6	0.0	CAC	−0.18		

We are grateful to Prof. Donald Bashford and to Dr. Bjoern Rabenstein for providing their programs MEAD and Karlsberg, respectively. We thank Dr. Laura Baciou for stimulating discussions.

A.T. is supported by a fellowship from the Deutscher Akademischer Austauschdienst (A/00/00063). G.M.U. is supported by a Emmy-Noether grant of the Deutsche Forschungsgemeinschaft (UL174/2-1). This work was supported by a PROCOPE program (DAAD/CNRS).

REFERENCES

Adcock, C., G. Smith, and M. Sansom. 1998. Electrostatics and the ion selectivity of ligand-gated channels. *Biophys. J.* 75:1211–1222.

Ädelroth, P., M. L. Paddock, L. B. Sagle, G. Feher, and M. Y. Okamura. 2000. indentification of the pathway in bacterial reaction centers: both protons associated with reduction of Q_B to Q_BH_2 share a common entry point. *Proc. Natl. Acad. Sci. USA*. 97:13086–13091.

Alexov, E., J. Miksovska, L. Baciou, M. Schiffer, D. K. Hanson, P. Sebban, and M. R. Gunner. 2000. Modeling the effects of mutations on the free energy of the first electron transfer from Q_A^- to Q_B in photosynthetic reaction centers. *Biochemistry*. 39:5940–5952.

Alexov, E. G., and M. R. Gunner. 1999. Calculated protein and proton motions coupled to electron transfer: electron transfer from Q_A^- to Q_B in bacterial photosynthetic reaction centers. *Biochemistry*. 38:8253–8270.

Allen, J. 1994. Crystallization of the reaction center from *Rhodobacter sphaeroides* in a new tetragonal form. *Proteins*. 20:283–286.

Baciou, L., and H. Michel. 1995. Interruption of the water chain in the reaction center from *Rhodobacter sphaeroides* reduces the rates of the proton uptake and of the second electron transfer to Q_B. *Biochemistry*. 34:7967–7972.

Baptista, A., and C. Soares. 2001. Some Theoretical and Computational Aspects of the Inclusion of Proton Isomerism in the Protonation Equilibrium of Proteins. *J. Phys. Chem. B*. 105:293–309.

Bashford, D., D. A. Case, C. Dalvit, L. Tennant, and P. E. Wright. 1993. Electrostatic calculations of side-chain pK_a values in myoglobin and comparison with NMR data for histidines. *Biochemistry*. 32:8045–8056.

Bashford, D., and K. Gerwert. 1992. Electrostatic calculations of the pK_a values of ionizable groups in bacteriorhodopsin. *J. Mol. Biol.* 224: 473–486.

Bashford, D., and M. Karplus. 1990. pK_a's of ionizable groups in proteins: atomic detail from a continuum electrostatic model. *Biochemistry*. 29:10219–10225.

Beroza, P., and D. A. Case. 1998. Calculations of proton-binding thermodynamics in proteins. *Methods Enzymol.* 295:170–189.

Beroza, P., D. R. Fredkin, M. Y. Okamura, and G. Feher. 1991. Protonation of interacting residues in a protein by a Monte Carlo method: application to lysozyme and the photosynthetic reaction center of *Rhodobacter sphaeroides*. *Proc. Natl. Acad. Sci. USA*. 88:5804–5808.

Beroza, P., D. R. Fredkin, M. Y. Okamura, and G. Feher. 1995. Electrostatic calculations of amino acid titration and electron transfer, $Q_A^-Q_B \rightarrow Q_AQ_B^-$, in the reaction center. *Biophys. J.* 68:2233–2250.

Brooks, B., R. Bruccoleri, B. Olafson, D. States, S. Swaminathan, and M. Karplus. 1983. CHARMM: A Program for Macromolecular Energy, Minimization, and Dynamics Calculations. *J. Comput. Chem.* 4:187–217.

Brunger, A. T., and M. Karplus. 1988. Polar hydrogen positions in proteins: empirical energy placement and neutron diffraction comparison. *Proteins*. 4:148–156.

Brzezinski, P., M. Y. Okamura, and G. Feher. 1992. Structural Changes Following the formation of $D^+Q_A^-$ in Bacterial Reaction centers: Measurement of Light-Induced Electrogenic Events in RCs Incorporated in a Phospholipid Bilayer. *In*: The Photosynthetic Bacterial Reaction Center II. J. B. A. Vermeglio, editor. Plenum Press, New York. 321–330

Chang, C., O. el-Kabbani, D. Tiede, J. Norris, and M. Schiffer. 1991. Structure of the membrane-bound protein photosynthetic reaction center from *Rhodobacter sphaeroides*. *Biochemistry*. 30:5352–5360.

Deisenhofer, J., O. Epp, K. Miki, R. Huber, and H. Michel. 1985. Structure of the protein subunits in the photosynthetic reaction center of *Rhodopseudomonas viridis* at 3Å resolution. *Nature*. 318:618–624.

Deisenhofer, J., and H. Michel. 1989. Nobel lecture. The photosynthetic reaction centre from the purple bacterium *Rhodopseudomonas viridis*. *EMBO J.* 8:2149–2170.

Ermler, U., G. Fritzsch, S. K. Buchanan, and H. Michel. 1994. Structure of the Photosynthetic Reaction Centre from *Rhodobacter sphaeroides* at 2.65 Å resolution: cofactors and protein-cofactor interactions. *Structure*. 2:925–936.

Gerencser, L., A. Taly, L. Baciou, P. Maroti, and P. Sebban. 2002. Cd^{2+} binding effect on bacterial reaction center mutants: the proton penetration involves interdependent pathways. *Biophys. J.* 80:518a. (Abstr.)

Gibas, C., and S. Subramaniam. 1996. Explicit solvent models in protein pK_a calculations. *Biophys. J.* 71:138–147.

Grafton, A. K., and R. A. Wheeler. 1999. Amino acid protonation states determine binding sites of the secondary ubiquinone and its anion in the *Rhodobacter sphaeroides* photosynthetic reaction center. *J. Phys. Chem. B*. 103:5380–5387.

Graige, M. S., G. Feher, and M. Y. Okamura. 1998. Conformational gating of the electron transfer reaction $Q_A^-Q_B \rightarrow Q_AQ_B^-$. in bacterial reaction centers of Rhodobacter sphaeroides determined by a driving force assay. *Proc. Natl. Acad. Sci. USA*. 95:11679–11684.

Gunner, M. R., and E. Alexov. 2000. A pragmatic approach to structure based calculation of coupled proton and electron transfer in proteins. *Biochim. Biophys. Acta*. 1458:63–87.

Hoffman, B. M., and M. A. Ratner. 1987. Gated electron transfer: when are observed rates controlled by conformational interconversion? *J. Am. Chem. Soc.* 109:6237–6243.

Honig, B., and A. Nicholls. 1995. Classical electrostatics in biology and chemistry. *Science*. 268:1144–1149.

Honig, B., K. Sharp, and M. Gilson. 1989. Electrostatic interactions in proteins. *Prog. Clin. Biol. Res.* 289:65–74.

Huang, Q., R. Opitz, E. W. Knapp, and A. Herrmann. 2002. Protonation and stability of the globular domain of influenza virus hemagglutinin. *Biophys. J.* 82:1050–1058.

Klapper, I., R. Fine, K. A. Sharp, and B. H. Honig. 1986. Focusing of electric fields in the active site of Cu-Zn superoxide dismutase: effects of ionic strength and amino-acid modification. *Proteins*. 1:47–59.

Kuglstatter, A., U. Ermler, H. Michel, L. Baciou, and G. Fritzsch. 2001. X-ray structure analyses of photosynthetic reaction center variants from *Rhodobacter sphaeroides*: structural changes induced by point mutations at position L209 modulate electron and proton transfer. *Biochemistry*. 40:4253–4260.

Lancaster, C. R. 1999a. Quinone-binding sites in membrane proteins: what can we learn from the *Rhodopseudomonas viridis* reaction centre? *Biochem. Soc. Trans*. 27:591–596.

Lancaster, C. R., M. V. Bibikova, P. Sabatino, D. Oesterhelt, and H. Michel. 2000. Structural basis of the drastically increased initial electron transfer rate in the reaction center from a *Rhodopseudomonas viridis* mutant described at 2.00-A resolution. *J. Biol. Chem.* 275:39364–39368.

Lancaster, C. R., and H. Michel. 1997. The coupling of light-induced electron transfer and proton uptake as derived from crystal structures of reaction centres from *Rhodopseudomonas viridis* modified at the binding site of the secondary quinone, Q_B. *Structure*. 5:1339–1359.

Lancaster, C. R., H. Michel, B. Honig, and M. R. Gunner. 1996. Calculated coupling of electron and proton transfer in the photosynthetic reaction center of *Rhodopseudomonas viridis*. *Biophys. J.* 70:2469–2492.

Lancaster, C. R. D. 1999b. The structure of the *Rhodopseudomonas viridis* reaction centre - an overview and recent advances. *In* Photosynthesis: Mechanisms and Effects. Vol 2. G. Garab, Editor, Kluwer, Dordrecht, NL. 673–678

Li, J., D. Gilroy, D. M. Tiede, and M. R. Gunner. 1998. Kinetic phases in the electron transfer from $P^+Q_A^-Q_B$ to $P^+Q_AQ_B^-$ and the associated processes in *Rhodobacter sphaeroides* R-26 reaction centers. *Biochemistry*. 37:2818–2829.

Maróti, P., and S. Osváth. 1997. Kinetics and energetics of photocycle in reaction center of photosynthetic bacteria. *Eur. Biophys. J*. 26:103.

Maroti, P., and C. A. Wraight. 1988. Flash-induced H^+ binding by bacterial photosynthetic reaction centers: influences of the redox states of the acceptor quinones and primary donor. *Biochim. Biophys. Acta*. 934:329–347.

McAuley, K. E., P. K. Fyfe, J. P. Ridge, R. J. Cogdell, N. W. Isaacs, and M. R. Jones. 2000. Ubiquinone binding, ubiquinone exclusion, and detailed cofactor conformation in a mutant bacterial reaction center. *Biochemistry*. 39:15032–15043.

McPherson, P. H., M. Y. Okamura, and G. Feher. 1988. Light-induced proton uptake by photosynthetic reaction centers from *Rhodobacter sphaeroides* R-26. I. Protonation of the one-electron states $D^+Q_A^-$, DQ_A^-, and $DQ_AQ_B^-$. *Biochim. Biophys. Acta*. 934:348–368.

Miksovska, J., L. Kálmán, M. Schiffer, P. Maróti, P. Sebban, and D. K. Hanson. 1997. In bacterial reaction centers rapid delivery of the second proton to Q_B can be achieved in the absence of L212Glu. *Biochemistry*. 36:12216–12226.

Mulkidjanian, A. Y. 1999. Conformationally controlled pK-switching in membrane proteins: one more mechanism specific to the enzyme catalysis? *FEBS Lett*. 463:199–204.

Nabedryk, E., J. Breton, R. Hienerwadel, C. Fogel, W. Mäntele, M. L. Paddock, and M. Y. Okamura. 1995. Fourier transforms infrared difference spectroscopy of secondary quinone acceptor photoreduction in proton transfer mutants of *Rhodobacter sphaeroides*. *Biochemistry*. 34:14722–14732.

Okamura, M. Y., M. L. Paddock, M. S. Graige, and G. Feher. 2000. Proton and electron transfer in bacterial reaction centers. *Biochim. Biophys. Acta*. 1458:148–163.

Onufriev, A., D. A. Case, and G. M. Ullmann. 2001. A novel view of pH titration in biomolecules. *Biochemistry*. 40:3413–3419.

Paddock, M. L., P. Adelroth, C. Chang, E. C. Abresch, G. Feher, and M. Y. Okamura. 2001. Identification of the Proton Pathway in Bacterial Reaction Centers: Cooperation between Asp-M17 and Asp-L210 Facilitates Proton Transfer to the Secondary Quinone (Q_B). *Biochemistry*. 40:6893–6902.

Rabenstein, B., and E. W. Knapp. 2001. Calculated pH-dependent population and protonation of carbon-monoxy-myoglobin conformers. *Biophys. J*. 80:1141–1150.

Rabenstein, B., G. M. Ullmann, and E. W. Knapp. 1998. Energetics of electron-transfer and protonation reactions of the quinones in the photosynthetic reaction center of *Rhodopseudomonas viridis*. *Biochemistry*. 37:2488–2495.

Rabenstein, B., G. M. Ullmann, and E. W. Knapp. 2000. Electron transfer between the quinones in the photosynthetic reaction center and its coupling to conformational changes. *Biochemistry*. 39:10487–10496.

Sebban, P., P. Maróti, and D. K. Hanson. 1995a. Electron and proton transfer to the quinones in bacterial photosynthetic reaction centers: insight from combined approaches of molecular genetics and biophysics. *Biochimie*. 77:677–694 [published erratum appears in *Biochimie*. 1995. 77:after table of contents].

Sebban, P., P. Maróti, M. Schiffer, and D. K. Hanson. 1995b. Electrostatic dominoes: long distance propagation of mutational effects in photosynthetic reaction centers of *Rhodobacter capsulatus*. *Biochemistry*. 34:8390–8397.

Sharp, K. A., R. A. Friedman, V. Misra, J. Hecht, and B. Honig. 1995. Salt effects on polyelectrolyte-ligand binding: comparison of Poisson-Boltzmann, and limiting law/counterion binding models. *Biopolymers*. 36:245–262.

Sharp, K. A., and B. Honig. 1990. Electrostatic interactions in macromolecules: theory and applications. *Annu. Rev. Biophys. Biophys. Chem*. 19:301–332.

Stowell, M. H., T. M. McPhillips, D. C. Rees, S. M. Soltis, E. Abresch, and G. Feher. 1997. Light-induced structural changes in photosynthetic reaction center: implications for mechanism of electron-proton transfer. *Science*. 276:812–816.

Sudmeier, J. L., and C. N. Reilley. 1964. Nuclear Magnetic Resonance Studies of Protonation of Polyamine and Aminocarboxylate Compounds in Aqueous Solution. *Anal. Chem*. 36:1698–1706.

Tandori, J., J. Miksovska, M. Valerio-Lepiniec, M. Schiffer, P. Maroti, D. K. Hanson, and P. Sebban. 2002. Proton Uptake of *Rhodobacter sphaeroides* Reaction Center Mutants Modified in The Primary Quinone Environment. *Photochem. Photobiol*. 75:126–133.

Tanford, C., and R. Roxby. 1972. Interpretation of protein titration curves. Application to lysozyme. *Biochemistry*. 11:2192–2198.

Teixeira, V., C. Soares, and A. Baptista. 2002. Studies of the reduction and protonation behavior of tetraheme cytochromes using atomic detail. *J. Biol. Inorg. Chem*. 7:200–216.

Tiede, D. M., and D. K. Hanson. 1992. Protein Relaxation Following Quinone Reduction in *Rhodobacter capsulatus*: Detection of Likely Protonation-Linked Optical Absorbance Changes of the Chromatophores. A. Vermeglio, editor. Plenum Press. New York. 341–350

Tiede, D. M., J. Vazquez, J. Cordova, and P. A. Marone. 1996. Time-resolved electrochromism associated with the formation of quinone anions in the *Rhodobacter sphaeroides* R26 reaction center. *Biochemistry*. 35:10763–10775.

Ullmann, G. M. 2000. The Coupling of Protonation and Reduction in Proteins with Multiple Redox centers. Theory, Computational Method, and Application to Cytochrome c_3. *J. Phys. Chem. B*. 104: 6293–6301.

Ullmann, G. M., and E. W. Knapp. 1999. Electrostatic models for computing protonation and redox equilibria in proteins. *Eur. Biophys. J*. 28:533–551.

Ullmann, G. M., E. W. Knapp, and N. M. Kostic. 1997. Computational Simulation and Analysis of the Dynamic Association between Plastocyanin and Cytochrome *f*. Consequences for the Electron-transfer Reaction. *J. Am. Chem. Soc*. 119:42–52.

Walden, S. E., and R. A. Wheeler. 2002. Protein Conformational Gate Controlling Binding Site Preference and Migration for Ubiquinone-B in the Photosynthetic Reaction Center of *Rhodobacter sphaeroides*. *J. Phys. Chem. B*. 106:3001–3006.

Wraight, C. A. 1979. Electron acceptors of bacterial photosynthetic reaction centers. II. H^+ binding coupled to secondary electron transfer in the quinone acceptor complex. *Biochim. Biophys. Acta*. 548: 309–327.

Yang, A. S., M. R. Gunner, R. Sampogna, K. Sharp, and B. Honig. 1993. On the calculation of pK_a*s* in proteins. *Proteins*. 15:252–265.

Zachariae, U., and C. R. Lancaster. 2001. Proton uptake associated with the reduction of the primary quinone Q_A influences the binding site of the secondary quinone Q_B in *Rhodopseudomonas viridis* photosynthetic reaction centers. *Biochim. Biophys. Acta*. 1505:280–290.

Zhou, J. S., and N. M. Kostic. 1993. Gating of photoinduced electron transfer from zinc cytochrome *c* and tin cytochrome *c* to plastocyanin. Effects of solution viscosity on rearrangement of the metalloprotein complex. *J. Am. Chem. Soc*. 115:10796–10804.

Zuiderweg, E. R., G. G. van Beek, and S. H. de Bruin. 1979. The influence of electrostatic interaction on the proton-binding behaviour of myo-inositol hexakisphosphate. *Eur. J. Biochem*. 94:297–306.